Article

pubs.acs.org/Biomac

Controlling Styrene Maleic Acid Lipid Particles through RAFT

Anton A. A. Smith,[†,‡,#] Henriette E. Autzen,[‡,§] Tomas Laursen,[∥,▽] Vincent Wu,[†] Max Yen,[†] Aaron Hall,[†] Scott D. Hansen,[⊥] Yifan Cheng,[§] and Ting Xu*[,†]

[†]Chemistry, Materials Science and Engineering UC Berkeley, Berkeley, California 94720, United States

[‡]Science and Technology, Aarhus University, 8000 Aarhus, Denmark

[§]Biochemistry and Biophysics, UCSF, San Francisco, California 94143, United States

[∥]Lawrence Berkeley National Laboratory, Berkeley, California 94720, United States

[⊥]California Institute for Quantitative Biosciences (QB3), UC Berkeley, Berkeley, California 94720, United States

Supporting Information

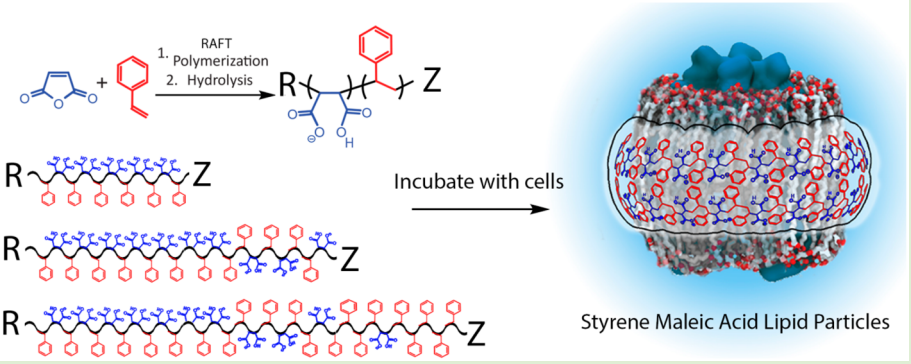

ABSTRACT: The ability of styrene maleic acid copolymers to dissolve lipid membranes into nanosized lipid particles is a facile method of obtaining membrane proteins in solubilized lipid discs while conserving part of their native lipid environment. While the currently used copolymers can readily extract membrane proteins in native nanodiscs, their highly disperse composition is likely to influence the dispersity of the discs as well as the extraction efficiency. In this study, reversible addition−fragmentation chain transfer was used to control the polymer architecture and dispersity of molecular weights with a high-precision. Based on Monte Carlo simulations of the polymerizations, the monomer composition was predicted and allowed a structure−function analysis of the polymer architecture, in relation to their ability to assemble into lipid nanoparticles. We show that a higher degree of control of the polymer architecture generates more homogeneous samples. We hypothesize that low dispersity copolymers, with control of polymer architecture are an ideal framework for the rational design of polymers for customized isolation and characterization of integral membrane proteins in native lipid bilayer systems.

INTRODUCTION

Integral membrane proteins remain some of the most challenging targets in structural biology and other related fields. Because of their hydrophobicity, membrane proteins are traditionally isolated and purified with detergents, forming protein detergent micelles. However, detergents pose a hazard for the protein stability and are an obstacle in their biophysical characterization. Furthermore, many membrane proteins are dependent on phospholipids to retain activity. Reconstituting integral membrane proteins into nanodiscs offers a solution to some of these challenges. The most prevalent method for obtaining membrane proteins in lipid nanodiscs is by reconstituting them into lipid nanodiscs with membrane scaffold proteins (MSPs). However, this method requires the membrane protein to be either partly or fully solubilized with detergents prior to reconstitution.[1,2] Not only is this route time-consuming, but it may also lead to protein destabilization and disassembly of protein complexes. Reconstitution also means a possible loss of important cofactors, which would be preserved in native nanodiscs. Despite all this, MSPs has gained popularity in single-particle cryo-electron microscopy (Cryo-EM) of membrane proteins.[1,3−6]

Styrene maleic acid (SMA) copolymers can solubilize lipid membranes and their components into nanoscale SMA lipid particles (SMALP), providing an efficient method for detergent-free solubilization of integral membrane proteins while obtaining them in solubilized discs (Figure 1).[7−9,8] The use of SMALPs has gained much interest in recent years, and applications include biochemical[10] and biophysical[11] characterization, as well as structural analysis through X-ray crystallography,[12] and single-particle Cryo-EM.[13,14] However, as the SMA copolymers currently available are adopted from

Received: August 8, 2017
Revised: September 19, 2017
Published: September 21, 2017

DOI: 10.1021/acs.biomac.7b01136
Biomacromolecules XXXX, XXX, XXX−XXX

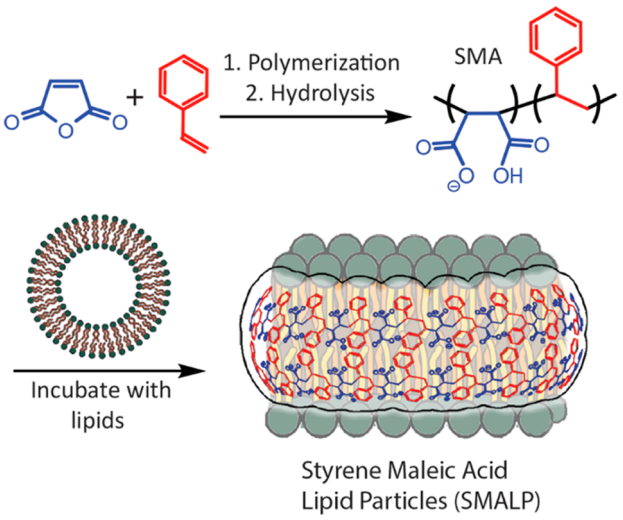

Figure 1. Synthesis of SMA and formation of SMALPs.

industrially used polymers, the designs are limited, and the field has yet to take advantage of modern polymerization techniques and the control of architecture they offer. Regardless, extraction of membrane proteins works with a disperse ensemble of polymer molecular weights.[7,8]

The SMA copolymer is produced by copolymerizing styrene (St) and maleic anhydride (MAnh), with subsequent hydrolysis of the anhydride copolymer (St-*co*-MAnh) yielding SMA (Figure 1). So far, the most effective polymers in terms of solubilizing lipids into discs have been found to have a styrene to maleic acid ratio of 2:1.[15] However, due to the alternating nature of this monomer pair, achieving a homogeneous distribution of the two monomers with this ratio is only possible through a continually stirring tank reactor (CSTR) at equilibrium.[16] However, CSTR made SMA is highly disperse in molecular weight, owing to its production via free-radical polymerization. Thus, obtaining a low dispersity of polymer molecular weights is not possible without fractionating the product through size exclusion chromatography (SEC). The steady state is necessarily maintained at approximately 97% St and ca. 3% MAnh to achieve the 2:1 ratio of St and MAnh in the resulting polymer. Any slight deviation will have a large effect on the resulting polymer composition. Consequently, the exact distribution of maleic acid along the polymer chain is typically unknown, as it requires deconvoluting quantitative ^{13}C NMR.[17−19] Therefore, studies using these polymers are limited by the assumption that the specific CSTR functions in an ideal manner.

St-*co*-MAnh polymers can also be made through RAFT polymerization, which lowers the dispersity of molecular weights.[20] However, RAFT polymerizations of St-*co*-MAnh will yield a gradient in the polymer composition as the ratio of monomer concentrations changes during the polymerization (Figure 2). This polymerization is a well-known method of making one-pot "block" copolymers.[17,18,21−23] In truth, these block copolymers are gradient copolymers with a very steep gradient as they change from alternating copolymers to a styrene homoblock. Here, we show that the gradient in the polymer composition can be modeled using the reactivity ratios determined by Klumpermann,[24] and thereby used to predict the compositions of RAFT made copolymers. Previous studies on SMALPs formed through RAFT made copolymers were performed assuming the polymerization was fully alternating so

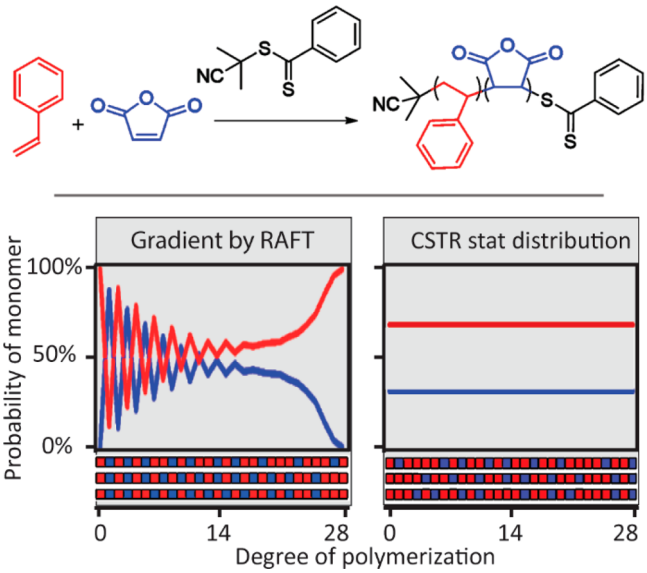

Figure 2. Simulations of the compositional drift in St-*co*-MAnh made by RAFT (left) compared to a hypothetical polymer of equal length made in a CSTR. The graph is the probability of finding St (red) or MAnh (blue) in a given monomer position in relation to the R group of the RAFT agent. Rows show examples of polymer composition over a given length, as obtained by simulation.

long as maleic anhydride was present.[25] This is an approximation which results in a loss of nuance in the understanding of the polymer composition. Modeling the reaction provides insight into the effects on polymer architecture yielded by changes to the experimental conditions, enabling a higher degree of control of the SMA system. Previous work with polymer self-assemblies, with and without protein, finds that global polymer composition, architecture and molecular weight all influence the self-assembled structures.[26−29] With this body of evidence, it can be assumed that these parameters can influence SMALPs, as these are self-assembled structures as well.

This work aims at establishing an understanding of which properties of the SMA copolymer architecture enable it to form SMALPs. By judiciously choosing polymerization conditions based on modeling the polymerization, we show that it is possible to control the molecular weight, the overall content of MAnh, as well as the extent of the gradient in monomer composition using the high-precision polymer synthesis RAFT. We show that a lower dispersity of the copolymer translates into a lower dispersity in SMALPs formed, offering a more homogeneous sample. We hypothesize that the control of SMALP dispersity will enable unprecedented structural studies of membrane proteins. This study also paves the way for new opportunities with SMALP systems in terms of conjugation chemistry, as the terminal functionality on the polymers can be used for highly controlled conjugations allowing addition of purification tags.

MATERIALS AND METHODS

Chemicals and Reagents. All reagents were purchased from Sigma-Aldrich and used without further purification unless specified otherwise. Azobisisobutryonitrile (AIBN) was recrystallized in ethanol prior to use. Inhibitor was removed from styrene prior to polymerization by cryo-distillation. Maleic anhydride was purified by sublimation under vacuum prior to polymerization.

DOI: 10.1021/acs.biomac.7b01136
Biomacromolecules XXXX, XXX, XXX−XXX

Simulations of Polymerizations. The polymerizations were simulated by the Monte Carlo method, using the penultimate model and the reactivity ratios determined by Klumperman et al.[24] An in-house program was made for determining compositions as a function of monomer conversion using the Mayo−Lewis equation, according to the method described by Harrison et al.[30] The program does not take the continuous initiation of polymers into account, and assumes all polymers to be of equal size. Additionally, polymers can add different number of monomers to the chain in each cycle of propagation. As a result, the composition of individual polymers can vary significantly from the average that the program predicts.[31] The polymerization should have a very selective addition to styrene by the cyanopropyl R group of the RAFT agent.[32] Accordingly, simulations were performed with the assumption that styrene was the first monomer to be added to the R group, regardless of MAnh concentration.

Polymerizations. Each reaction mixture was divided equally between 6 clean 50 mL glass Schlenk tubes fitted with Teflon screw caps. The reaction mixtures were degassed by 4 freeze−pump−thaw cycles and sealed at 30 mTorr. All polymerizations were heated to 70 °C for the duration of the polymerization. Polymers were purified by precipitation into isopropanol, followed by filtering the polymers and drying in vacuo. This yielded the polymers as pink powders. The table containing all measured conversions is in Table S1.

A series: [M]:[RAFT] = 400, [St]:[MAh] = 95:5. A stock solution of the reaction mixture was prepared by mixing styrene (32.6 g, 313 mmol), maleic anhydride (1.62 g, 16.5 mmol), 2-cyano-2-propyl benzodithioate (180 mg, 0.81 mmol), AIBN (27 mg, 0.16 mmol), and DMF (32.7 g, 31.0 mL). Individual reactions polymerized for 1−4 h (A1), 5 h (A2), and 16 h (A3).

B series: [M]:[RAFT] = 200, [St]:[MAh] = 90:10. A stock solution of the reaction mixture was prepared by mixing styrene (31.0 g, 297 mmol), maleic anhydride (3,24 g, 33.0 mmol), 2-cyano-2-propyl benzodithioate (350 mg, 1.60 mmol), AIBN (51 mg, 0.32 mmol), and DMF (30.9 g, 29.3 mL). Individual reactions polymerized for 2, 4 h (B1), 6 h (B2), 8 h (B3), 10 h (B4) and 16 h (B5).

C series: [M]:[RAFT] = 100, [St]:[MAh] = 80:20. A stock solution of the reaction mixture was prepared by mixing styrene (27.4 g, 220 mmol), maleic anhydride (6.46 g, 65.9 mmol), 2-Cyano-2-propyl benzodithioate (738 mg, 3.33 mmol), AIBN (0.11 mg, 0,66 mmol), and DMF (27.5 g, 26: mL). Individual reactions polymerized for 2, 4 (C1), 6 (C2), 8 (C3), 10 (C4) and 16 h (C5).

D [M]:[RAFT] = 43, [St]:[MAh] = 3:1. The reaction mixture was prepared by mixing styrene (2.66 g, 25.6 mmol), maleic anhydride (536 mg, 8.5 mmol), 2-Cyano-2-propyl benzodithioate benzodithioate (176 mg, 894 μmol), AIBN (26 mg, 0.16 mmol), and Dioxane (2.9 mL). This reaction polymerized for 16 h.

E [M]:[RAFT] = 43, [St]:[MAh] = 2:1. The reaction mixture was prepared by mixing styrene (2.36 g, 23 mmol), maleic anhydride (1.11 g, 11.3 mmol), 2-cyano-2-propyl benzodithioate (176 mg, 894 μmol), AIBN (26 mg, 0.16 mmol), and dioxane (2.6 mL). This reaction polymerized for 16 h.

F [M]:[RAFT] = 92, [St]:[MAh] = 3:1. The reaction mixture was prepared by mixing styrene (2.66 g, 25.6 mmol), maleic anhydride (536 mg, 8.5 mmol), 2-cyano-2-propyl benzodithioate (82.4 mg, 0.372 mmol), AIBN (12 mg, 75 μmol), and dioxane (2.9 mL). This reaction polymerized for 16 h.

Hydrolysis of St-*co*-MAnh. Conversion of St-*co*-MAnh to SMA was performed by hydrolysis in THF. Here 500 mg of polymer was dissolved in 4 mL of THF, 2 mL of water and 1 mL of TEA in a 50 mL tube. This initially dissolved the polymer. A cloudy suspension formed after a few minutes and fully phase separated after 30 min at 70 °C. The hydrolyzed polymer was then precipitated by the addition of water and HCl(aq). Centrifuging the precipitate was followed by decanting off the supernatant, and the polymer was further purified by dissolving the precipitate in a minimum of ethanol, followed by reprecipitation by the addition of water. This procedure was repeated three times and the purified product was dried in vacuo. This procedure hydrolyzed the anhydride, yet preserved the terminal dithiobenzoate. Using NaOH for the hydrolysis resulted in the dithiobenzoate being partially cleaved.

One-Pot Maleimide Functionalization. The dithiobenzoate was cleaved from the sodium-salt of polymers with 5 equiv of butylamine, in the presence of 5 equiv trimethylphosphite in methanol at a concentration of 50 mg/mL of polymer. This reaction was determined to be complete by ^{1}H NMR after 28 h at room temperature (Figure S1). Next, 2.5 equiv of sulfo-cyanine5 maleimide was added and left to react overnight. Conjugated products were recovered by evaporating the methanol with a gentle air flow, followed by dissolving the crude product in water. This was passed twice through Illustra NAP columns and lyophilized to yield the polymer conjugate. Coelution of dye and polymer on the NAP column proved a successful conjugation.

To show the conjugation by ^{1}H NMR, a sample polymer was purified after dithiobenzoate removal by precipitation into 0.1 M HCl (aq) and washing with water, and then residual water was removed in vacuo. This sample was subsequently dissolved in MeOD with 0.05 M K_2CO_3, with 2.5 equiv *N*-methyl maleimide subsequently being added, yielding the maleimide conjugate. Comparing the polymer conjugate with the nonconjugated polymer by ^{1}H NMR revealed approximately 86% of the polymer end groups had been modified with the maleimide.

Characterization of Copolymers. ^{1}H NMR spectra were carried with a Bruker Avance DRX 500 spectrometer (500 MHz) using a 5 mm Z-gradient Broad Band probe or a Bruker Avance AV 500 spectrometer (500 MHz) using a Z-gradient Triple Broad Band Inverse detection probe. Styrene conversion was measured on crude reaction mixtures in CDCl3, using DMF as an internal standard. The calculated styrene content from the conversions combined with the simulations was compared to the styrene to maleic acid ratio found in purified SMA in MeOD. Number-average (M_n) and weight-average (M_w) molar mass and dispersity ($Đ = M_w/M_n$) of copolymers were obtained from gel permeation chromatography (GPC) carried out using an Agilent 1260 Infinity series instrument outfitted with an Agilent PolyPore column (300 × 7.5 mm). THF was used as eluent at 1 mL min^{-1} at room temperature. Poly(methyl methacrylate) standards were used to calibrate the GPC system. Analyte samples at 2 mg mL^{-1} were filtered through a polytetrafluoroethylene (PTFE) membrane with 0.2 mm pore before injection (20 μL).

Lipid solubilization assay. For each sample, 10 μL of POPC with 2% of Liss Rho PE and 10 μL of a 10 wt % neutralized polymer solution and 80 μL of HEPES buffer pH 7.3 to a total volume of 100 μL. The samples were incubated for 30 min at 30 °C and 700 rpm. Nonsolubilized lipid was removed by centrifugation at 20 000*g* for 30 min. The absorption of Liss Rho PE was measured at 550 nm to quantify solubilized lipid. Size exclusion chromatography of SMALPs was performed on an ÄKTA explorer 100 FPLC system (GE Life Sciences) equipped with a Superose 6 10/300 GL column (GE Life Sciences) and a flow rate of 0.5 mL min^{-1}. The column was pre-equilibrated in running buffer (50 mM HEPES, 100 mM NaCl pH 7.0).

Membrane Protein Extraction and Fluorescence-SEC Analysis. Here 25 mg of HEK293F cells expressing a GFP-tagged membrane protein were resuspended in 200 μL HBS (50 mM HEPES, pH 7.4 and 150 mM NaCl) supplemented with EDTA-Free SIGMAFAST Protease Inhibitor Cocktail tablets (Sigma). Next 50 μL of cell suspension was mixed with 50 μL of 2% polymer solubilized in HBS for a final concentration of 1% and incubated on a rolling table for 2 h. Large aggregates were removed from the suspension by ultracentrifugation at 70 000*g* for 10 min and 10 μL of the supernatant was loaded onto a Superose6 column (5/150 GL) pre-equilibrated with HBS buffer. Separation was performed at a flow rate of 0.2 mL/min, and the eluent was detected by using a Shimadzu fluorometer with excitation at 488 nm, emission at 509 nm, and a recording time of 20 min.

Microscope Hardware and Imaging Acquisition. Single SMA lipid particles containing a mixture of SMA-D, 98% 1-palmitoyl-2-oleoyl-*sn*-glycero-3-phosphocholine (16:0−18:1 POPC, Avanti Polar Lipids cat# 850457), and 2% Lissamine Rhodamine phosphoethanolamine (16:0 Liss Rhod PE, Avanti Polar Lipids cat# 810158) were visualized on an inverted Nikon Eclipse Ti microscope using a Nikon 100× TIRF oil immersion objective (1.49 NA). Samples were

DOI: 10.1021/acs.biomac.7b01136
Biomacromolecules XXXX, XXX, XXX−XXX

positioned in the *x*-axis and *y*-axis using an Applied Scientific Instrumentation (ASI) stage and joystick. Images were acquired on an Andor iXon Ultra EMCCD camera (Andor Technology Ltd., UK). Fluorescent SMA lipid particles were excited using a 561 nm diode laser (OBIS laser diode, Coherent Inc. Santa Clara, CA) controlled with a Solemere laser driver with analog and digital modulation (~2 mW of power measured through the objective). Excitation light was passed through a dichroic filter cube (ZT561rdc, Semrock), followed by ET600/50M (Semrock) mounted in a Sutter Instruments filter wheel. TIRF microscopy images of SMA lipid particles were collected at 21−23 °C in phosphate buffer saline [pH 7.4]. Microscope and hardware were controlled using Micro-Manager v4.0.[33]

Particle Intensity Distribution and Multistep Photobleaching. Using ImageJ, TIRF microscope images of SMA lipid particles were converted from 16-bit to 8-bit files. Images were the thresholded, despeckled, and converted to a binary mask representing the position of each SMA lipid particle. Measurements were set to integrate the intensity of each particle on the raw data file using the binary mask for particle coordinates. Histogram of SMA lipid particles intensities was generated using PRISM graphing software. Representative SMA lipid particle multistep-photobleaching trace (Figure 6C) was generated in ImageJ using the *Z*-axis profile tool to measure the integrated intensity as a function of time.

RESULTS AND DISCUSSION

RAFT Polymerization of St-*co*-MAnh Copolymers. In order to control size, dispersity, polymer composition, and statistical distribution of momoners, we employed RAFT polymerization. The experimental conditions were chosen on the basis of simulations using the Mayo−Lewis equation,[34] including the penultimate monomer model and reactivity ratios for the copolymerization.[24] While the modeling is mathematically very simple, there is a gap between experimentalists and theoreticians, as there are very few practical tools to model polymerizations. Inspired by the work of Harrison et al.,[30] we developed an easy to use in-house program, capable of modeling compositional drifts in controlled radical polymerizations, based on the ratio between individual monomers ([St]:[MAnh]), monomers to RAFT ([M]:[RAFT]), and reactivity ratios of the monomers. This program is the focus of a future publication.

Our simulations show a gradient in the composition, yet using a high [M]:[RAFT] ratio along with a very large [St]:[MAnh] ratio would result in a high styrene fraction at low degree of polymerization (DP) with only a slight gradient in compositional drift. Decreasing the [St]:[MAnh] ratio while decreasing the [M]:[RAFT] ratio results in polymers with a greater gradient in composition, but a similar, albeit DP dependent, composition globally. In addition to these, select samples were made aiming for low DP polymers with a very steep gradient in compositional drift. Altogether, by varying the experimental parameters on the basis of the simulations, it was possible to control MAnh content as well as the compositional gradient, Figure 3 and Table S1. There were a few noteworthy observations during the synthesis of the polymers: aqueous solutions of SMA polymers terminated while MAnh was still present in the reaction mixture appear amber in color, while those terminated after MAnh depletion are pink (Figure 4).

The change in color in the B series supports that MAnh is the terminal group on dormant chains while it is still present in the polymerization, due to the MAnh radical having a high affinity toward the C═S bond.[16] In addition to the styrene content following the trend predicted by simulation (Table S1). ^{1}H NMR also supports the change in compositional drift. As the polymerization progresses a shoulder emerges in the phenyl

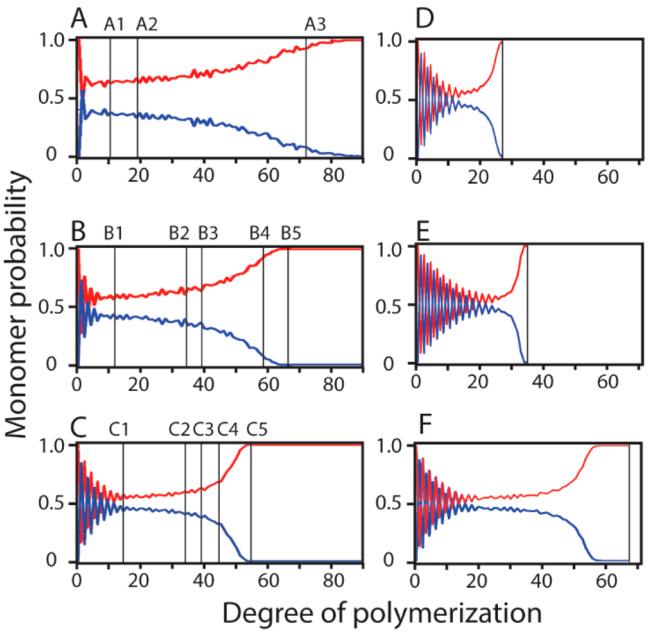

Figure 3. Compositional trajectories with different [M]:[RAFT] and [St]:[MAnh] ratios. Probabilities are denoted in the plot, St (red), MAnh (blue). Individual polymers within a set reached different conversions by stopping the reactions at different time points. A vertical line indicates a synthesized polymer described in Table S1. Simulations are performed with styrene being the first monomer, according to the reactivity of the cyanoisopropyl radical.

peak shape at 6.6 ppm, corresponding to more nonalternating styrene segments (Figure 4). ^{13}C NMR of these polymers also corroborates the emergence of SSS triads (data not shown). However, as MAnh is depleted, the rate of propagation slows. Consequently, growing a styrene homoblock takes significantly longer than a statistical copolymer block.[35] All methods of analysis support RAFT control, i.e., size determined by GPC, the [St]:[MAnh] ratio determined by ^{1}H NMR of the purified polymer, and the presence of the dithiobenzoate end group. For each polymer series, higher monomer conversions via ^{1}H NMR yielded correspondingly higher molecular weights via GPC. Thus, using the reactivity ratios, it is possible to predict and aim for specific compositions with RAFT polymerization, affording an entire new dimension of control. This allows for RAFT produced polymers that approximate the statistical distribution of CSTR made polymers, while maintaining low dispersity in molecular weight. The trade-off to this approach is that this control is only allowed in a narrow window in terms of DP, i.e., high DP low dispersity polymers with regularly dispersed MA are not possible through this technique. This set of polymers allows to assay the importance of individual parameters, by comparing polymers that only differ in one parameter (e.g., global styrene content, gradient, and DP).

Terminal Conjugation. The polymers were shown to be terminally functionalized through facile thiol-maleimide coupling. SMALPs have previously been functionalized with cysteamine, opening the anhydride to yield thiols as pendant groups.[36] While functional, the drawback is that nonstoichiometric pendant group functionalization adds functional group dispersity to a system already highly disperse in molecular weight. Functionalization through the RAFT terminal groups allows for a controlled conjugation with a single moiety per polymer. By virtue of the RAFT polymerization, the polymers

DOI: 10.1021/acs.biomac.7b01136
Biomacromolecules XXXX, XXX, XXX−XXX

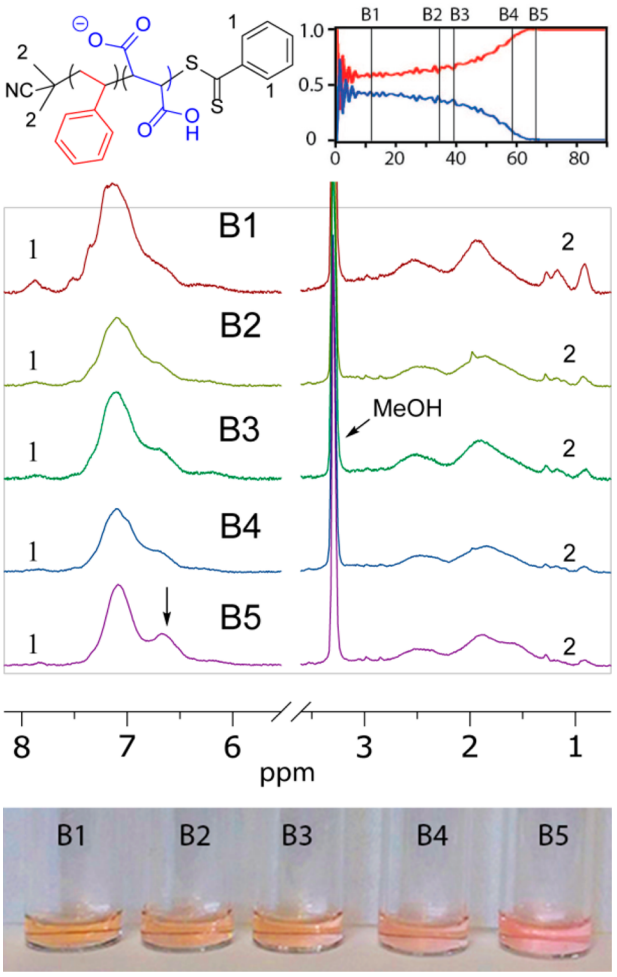

Figure 4. [1]H NMR of B series in MeOD. As end groups constitute less of the polymer mass as the polymerization proceeds they also recede in intensity (1 and 2). Additionally, a shoulder on the phenyl signal increases in intensity as the styrene content increases, arising from nonalternating styrene segments. Bottom: colors of SMA solutions, showing a shift from amber to pink as styrene becomes the dominating terminal residue.

have a dithiobenzoate terminus after gentle hydrolysis of the maleic anhydride. This can be removed and the resulting thiol can be sequentially coupled to a maleimide in a one-pot reaction, Scheme 1. Abel and McCormick describe the one-pot terminal functionalization of RAFT made polymers using maleimides,[37] and the reaction was accommodated to this polymer system. In short, butylamine was allowed to react with the sodium salt of the hydrolyzed polymer in methanol to cleave the dithiobenzoate (Figure S1). The reaction was performed in the presence of trimethylphosphite to protect the formed thiol from oxidation. Subsequently, *N*-methyl maleimide was added, yielding the conjugate in less than 1 h, with approximately 86% of the polymers having been functionalized with the maleimide. The applicability of this coupling chemistry in conjunction with SMALP formation is broad, yet easy to approach as functional maleimides are widely available. This feature of the polymers could have ramifications well beyond this work.

SMALP Formation. It is observed that both global styrene content as well as composition influence the ability to dissolve lipids (Figure 5A). Scheidelaar et al. describe that the property necessary for SMALP formation is essentially the amphiphilicity of the polymer, with the 2:1 ratio of [St]:[MA] being the most effective. Correspondingly, a higher content of MA still proves useful at lower pH, as the carboxylates are partially protonated thereby canceling out some of the charge of the polymer, corroborating their conclusion that the overall amphiphilicity is pivotal. It was also clear that polymers were ineffective at pH 7.3 when comparing the C series to polymers B1−B4, with the main difference between the two series being the MA content.

A gradient statistical distribution of MA in RAFT made SMA does seem to be beneficial, as seen with D being superior to B3. Both polymers have similar MA content and size, but a different gradient in composition.

However, if the polymerization proceeds beyond the gradient, as is observed for B5, the ability to solubilize lipids is diminished. The polymer that exhibited the highest solubilizing ability was D, a polymer of only 3 kDa, with a very steep gradient in composition. So while size does not seem to carry any influence with polymers of a homogeneous composition, a small polymer with a steep gradient appears to be more effective than a polymer of similar size and MA content, but lacking the strong gradient, such as B2 and B3. The lipid particles for the different successful polymers were further analyzed by SEC, measuring the absorbance of Liss Rho PE.

Scheme 1[a]

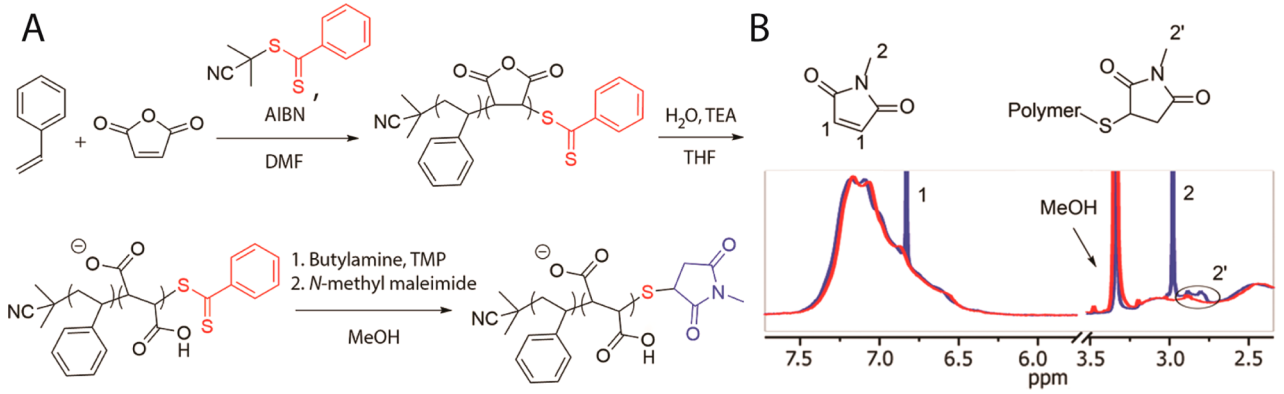

[a](A) Polymerization and one-pot maleimide conjugation. (B) [1]H NMR of polymer prior to conjugation (red line) and after conjugation with excess maleimide (blue line).

DOI: 10.1021/acs.biomac.7b01136
Biomacromolecules XXXX, XXX, XXX−XXX

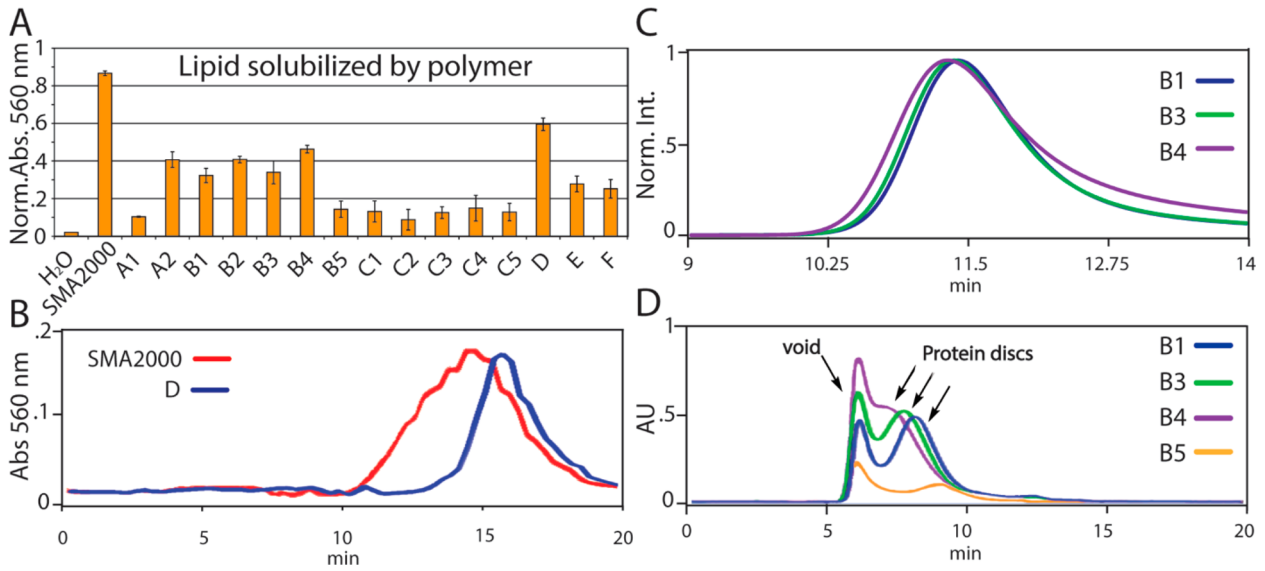

Figure 5. (A) Lipid dissolution. Ability to solubilize a mixture of Liss Rho PE with DOPC, normalized to lipid solubilized with Triton X. The conditions of the assay were chosen so SMA2000 did not solubilize all lipid, as to give a comparison of the lipid solubilizing capabilities of the RAFT polymers in relation to the maximum capacity of SMA2000. Of all the polymers tested, the commercially available SMA2000 solubilized the most lipid. A1 was ineffective in comparison to A2. The B series dissolves more lipid than C series, expected from the higher styrene content. B5 is comparable to the C series, despite having the highest styrene content of the B series. Of the RAFT made polymers D was most effective lipid solubilizer. (B) SEC of discs made with SMA2000 and SMA-D, with SMA-D showing low dispersity of discs formed. (C) FSEC of lipid particles with Liss Rho PE, showing discrete SMALP sizes, from smallest to largest; B1 < B3 < B4. B2 is omitted for clarity as B2 and B3 produced similar sizes. (D) FSEC of GFP-fused membrane protein in discs made with the B series. B1, B3, and B4 yield distinct disc sizes. From the change in elution time, it is observed that the modest differences in size observed in empty discs are amplified by the inclusion of protein in the discs. B5 was not capable of producing discs.

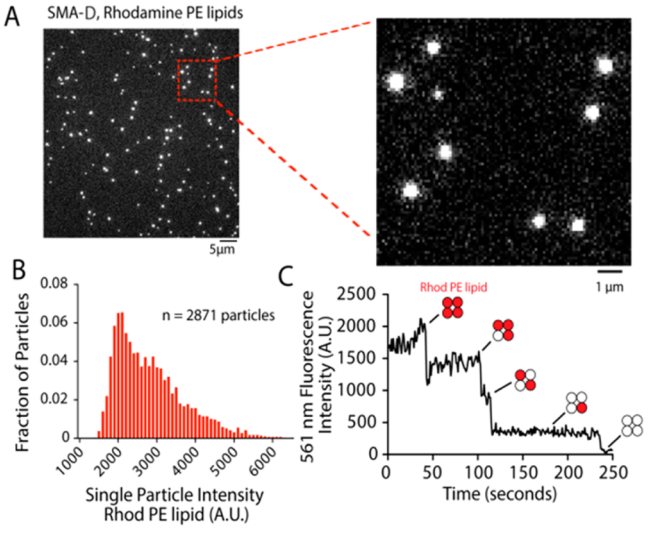

Figure 6. Visualization of RAFT polymer D lipid particles by fluorescence microscopy. (A) Fluorescence microscopy image of lipid particles generated in the presence of polymer D. Magnified image of fluorescent particles shown to the right. (B) Frequency distribution of lipid particle intensity. Measurements represents mean fluorescence intensity of individual particles (n = 2871 particles analyzed). (C) Lipid composition: 98% POPC, 2% Rhodamine PE.

The polymer D yielded a narrow dispersity of particle sizes in comparison with SMA2000 (Figure 5B). The fact that polymers with a well-defined architecture and low dispersity yield low-dispersity particles shows that a fine degree of control of SMALP sizes is possible. The polymers B1−B4 made SMALPs with both narrow dispersity and discrete sizes across the series (Figure 5C), while B5 was ineffective in producing SMALPs. Although, SEC demonstrates that discs generated in the presence of polymer D are of very low dispersity (Figure 5B), variability in disc fluorescent intensity is observed (Figure 6A); this can be attributed to Poissonian distribution of Rhodamine PE lipids (Figure 6B) across all discs formed. Multistep photobleaching confirms the number of fluorescent lipids in individual discs (Figure 6C).

Structural biology applications are expected to benefit from lower sample dispersity. Initial testing of these polymers has been performed with an oligomeric membrane protein of which a structure has yet to be elucidated. The polymer was added to a suspension of whole cells to solubilize the protein directly with native lipids. The size of the protein-SMALP varies with the polymer used, showing that the control of size is also possible in the presence of protein (Figure 5D). Surprisingly, polymers C1−C4 were effective and all made particles of similar sizes (Figure S2), showing that an inability of polymers to dissolve lipids does not necessarily translate into an incapability to solubilize membrane proteins. Moreover, it was observed that polymers harboring a short styrene homoblock, B5, C5, and F, were completely incapable of dissolving protein into SMALPs. Here the observations regarding lipid dissolution coincide with the lack of ability to make protein containing SMALPs, adding weight to the observation that a styrene homoblock is detrimental to the system. Polymer D is the interesting exception, being very small while having a very sharp gradient and an average terminal sequence of 2−3 styrene residues, which hardly qualifies as a block. With these properties, D has more features in common with classic detergents than it does with SMA2000. The fact that D was the most effective SMA copolymer demonstrates that efficient SMALP forming polymers can have properties that deviate substantially from the most commonly used SMA

DOI: 10.1021/acs.biomac.7b01136
Biomacromolecules XXXX, XXX, XXX−XXX

copolymers Taken together with the new possibilities involving terminal conjugations, it is fortunate that D proved effective. Short polymers allow for more functionalization per mass. However, given its small size, the ability to form SMALPs could be affected, as any tag conjugate will result in a change in polymer structure. This will likely be case specific, and a longer polymer with less of a gradient would likely be preferred if this is an issue for the smaller polymers.

CONCLUSIONS

By combining simulation with meticulous RAFT polymer synthesis, it is possible to make well-defined SMA copolymers having control of size and polymer architecture in terms of both composition and their drift along the polymer chain. These polymers were in turn shown to dissolve lipids and form SMALPs, with and without integral membrane protein. The system is flexible in terms of variations in polymer architecture. The size of the polymer did not show an effect if the global composition was comparable; however, a styrene homoblock was in most cases detrimental to the system. The size of protein containing SMALPs can likely be controlled through a combination of size and slope of the gradient in its composition, as was found for the B series of polymers. The SMALPs made through low-dispersity polymers also exhibit a lower dispersity than SMA2000. Finally, the RAFT technique allows controlled conjugations to maleimides through the polymer terminus; a feat not possible on commercially available SMA polymers. This allows for functionalization with dyes and affinity tags, increasing the utility of RAFT made SMA. This is in line with the needs of the system molecular biology, as it transforms SMA nanodiscs into a tool with fewer uncertainties, as the system attains a lower dispersity of all properties.

ASSOCIATED CONTENT

Supporting Information

The Supporting Information is available free of charge on the ACS Publications website at DOI: 10.1021/acs.biomac.7b01136.

All measured polymer properties; ^{1}H NMR removal of dithiobenzoate of polymer D; FSEC of GFP fused membrane protein with C series (PDF)

AUTHOR INFORMATION

Corresponding Author

*E-mail: tingxu@berkeley.edu.

ORCID

Anton A. A. Smith: 0000-0001-6728-5299

Ting Xu: 0000-0002-2831-2095

Present Addresses

#A.A.A.S.: Materials Science and Engineering, Stanford University, Stanford, CA 94305, USA.

∇T.L.: Department of Plant and Environmental Sciences, University of Copenhagen, 1017 Copenhagen, Denmark.

Author Contributions

The manuscript was written through contributions of all authors. All authors have given approval to the final version of the manuscript.

Notes

The authors declare no competing financial interest.

ACKNOWLEDGMENTS

A.A.A.S is the recipient of a postdoc scholarship from the Danish Council of Independent Research (Grant No. DFF-5054-00215). H.E.A is the recipient of a postdoc scholarship from the Danish Council of Independent Research (Grant No. DFF-5051-00085). T.L. is the recipient of a postdoc fellowship awarded by the VILLUM Foundation (Project No. 95-300-73023). The work was supported by Department of Defense, Army Research Office under contract W911NF-13-1-0232.

ABBREVIATIONS

St, styrene; MAnh, maleic anhydride; SMA, styrene maleic acid; MA, maleic acid; CSTR, continually stirring tank reactor; M, monomer; RAFT, reversible addition−fragmentation chain transfer; SMALP, styrene maleic acid lipid particle; SEC, size exclusion chromatography; FSEC, fluorescence size exclusion chromatography; GFP, green fluorescent protein; THF, Tetrahydrofurane; TEA, Triethylamine

REFERENCES

(1) Denisov, I. G.; Sligar, S. G. Nanodiscs for structural and functional studies of membrane proteins. *Nat. Struct. Mol. Biol.* **2016**, *23* (6), 481−486.

(2) Schuler, M. A.; Denisov, I. G.; Sligar, S. G. Nanodiscs as a new tool to examine lipid-protein interactions. *Methods Mol. Biol.* **2013**, *974*, 415−33.

(3) Denisov, I. G.; Sligar, S. G. Nanodiscs in Membrane Biochemistry and Biophysics. *Chem. Rev.* **2017**, *117* (6), 4669−4713.

(4) Gao, Y.; Cao, E. H.; Julius, D.; Cheng, Y. F. TRPV1 structures in nanodiscs reveal mechanisms of ligand and lipid action. *Nature* **2016**, *534* (7607), 347−351.

(5) Shen, P. S.; Yang, X. Y.; DeCaen, P. G.; Liu, X. W.; Bulkley, D.; Clapham, D. E.; Cao, E. H. The Structure of the Polycystic Kidney Disease Channel PKD2 in Lipid Nanodiscs. *Cell* **2016**, *167* (3), 763.

(6) Efremov, R. G.; Leitner, A.; Aebersold, R.; Raunser, S. Architecture and conformational switch mechanism of the ryanodine receptor. *Nature* **2015**, *517* (7532), 39−U72.

(7) Dafforn, T. R.; Jamshad, M.; Lin, Y. P.; Knowles, T. J.; Wheatley, M.; Poyner, D. R.; Bill, R. M.; Parslow, R.; Thomas, O. R. Detergent-free purification of membrane proteins. *Abstr. Pap Am. Chem. Soc.* **2012**, 243.

(8) Lee, S. C.; Knowles, T. J.; Postis, V. L. G.; Jamshad, M.; Parslow, R. A.; Lin, Y. P.; Goldman, A.; Sridhar, P.; Overduin, M.; Muench, S. P.; Dafforn, T. R. A method for detergent-free isolation of membrane proteins in their local lipid environment. *Nat. Protoc.* **2016**, *11* (7), 1149−1162.

(9) Oluwole, A. O.; Danielczak, B.; Meister, A.; Babalola, J. O.; Vargas, C.; Keller, S. Solubilization of Membrane Proteins into Functional Lipid-Bilayer Nanodiscs Using a Diisobutylene/Maleic Acid Copolymer. *Angew. Chem., Int. Ed.* **2017**, *56* (7), 1919−1924.

(10) Laursen, T.; Borch, J.; Knudsen, C.; Bavishi, K.; Torta, F.; Martens, H. J.; Silvestro, D.; Hatzakis, N. S.; Wenk, M. R.; Dafforn, T. R.; Olsen, C. E.; Motawia, M. S.; Hamberger, B.; Moller, B. L.; Bassard, J. E. Characterization of a dynamic metabolon producing the defense compound dhurrin in sorghum. *Science* **2016**, *354* (6314), 890−893.

(11) Pardo, J. J. D.; Dorr, J. M.; Iyer, A.; Cox, R. C.; Scheidelaar, S.; Koorengevel, M. C.; Subramaniam, V.; Killian, J. A. Solubilization of lipids and lipid phases by the styrene-maleic acid copolymer. *Eur. Biophys. J.* **2017**, *46* (1), 91−101.

(12) Broecker, J.; Eger, B. T.; Ernst, O. P. Crystallogenesis of Membrane Proteins Mediated by Polymer-Bounded Lipid Nanodiscs. *Structure* **2017**, *25* (2), 384−392.

(13) Postis, V.; Rawson, S.; Mitchell, J. K.; Lee, S. C.; Parslow, R. A.; Dafforn, T. R.; Baldwin, S. A.; Muench, S. P. The use of SMALPs as a novel membrane protein scaffold for structure study by negative stain

DOI: 10.1021/acs.biomac.7b01136
Biomacromolecules XXXX, XXX, XXX−XXX

electron microscopy. *Biochim. Biophys. Acta, Biomembr.* **2015**, *1848* (2), 496−501.
(14) Smirnova, I. A.; Sjostrand, D.; Li, F.; Bjorck, M.; Schafer, J.; Ostbye, H.; Hogbom, M.; von Ballmoos, C.; Lander, G. C.; Adelroth, P.; Brzezinski, P. Isolation of yeast complex IV in native lipid nanodiscs. *Biochim. Biophys. Acta, Biomembr.* **2016**, *1858* (12), 2984−2992.
(15) Scheidelaar, S.; Koorengevel, M. C.; Pardo, J. D.; Meeldijk, J. D.; Breukink, E.; Killian, J. A. Molecular Model for the Solubilization of Membranes into Nanodisks by Styrene Maleic Acid Copolymers. *Biophys. J.* **2015**, *108* (2), 279−290.
(16) Klumperman, B. Mechanistic considerations on styrene-maleic anhydride copolymerization reactions. *Polym. Chem.* **2010**, *1* (5), 558−562.
(17) Yao, Z.; Zhang, J. S.; Chen, M. L.; Li, B. J.; Lu, Y. Y.; Cao, K. Preparation of Well-Defined Block Copolymer Having One Polystyrene Segment and Another Poly(styrene-alt-maleic anhydride) Segment with RAFT Polymerization. *J. Appl. Polym. Sci.* **2011**, *121* (3), 1740−1746.
(18) Lessard, B.; Maric, M. One-Step Poly(styrene-alt-maleic anhydride)-block-poly(styrene) Copolymers with Highly Alternating Styrene/Maleic Anhydride Sequences Are Possible by Nitroxide-Mediated Polymerization. *Macromolecules* **2010**, *43* (2), 879−885.
(19) Ha, N. T. H. Determination of triad sequence distribution of copolymers of maleic anhydride and its derivates with donor monomers by C-13 nmr spectroscopy. *Polymer* **1999**, *40* (4), 1081−1086.
(20) Chiefari, J.; Chong, Y. K.; Ercole, F.; Krstina, J.; Jeffery, J.; Le, T. P. T.; Mayadunne, R. T. A.; Meijs, G. F.; Moad, C. L.; Moad, G.; Rizzardo, E.; Thang, S. H. Living free-radical polymerization by reversible addition-fragmentation chain transfer: The RAFT process. *Macromolecules* **1998**, *31* (16), 5559−5562.
(21) Benoit, D.; Hawker, C. J.; Huang, E. E.; Lin, Z. Q.; Russell, T. P. One-step formation of functionalized block copolymers. *Macromolecules* **2000**, *33* (5), 1505−1507.
(22) Han, J. T.; Silcock, P.; McQuillan, A. J.; Bremer, P. Preparation and characterization of poly(styrene-alt-maleic acid)-b-polystyrene block copolymer self-assembled nanoparticles. *Colloid Polym. Sci.* **2008**, *286* (14−15), 1605−1612.
(23) Baranello, M. P.; Bauer, L.; Benoit, D. S. W. Poly(styrene-alt-maleic anhydride)-Based Diblock Copolymer Micelles Exhibit Versatile Hydrophobic Drug Loading, Drug-Dependent Release, and Internalization by Multidrug Resistant Ovarian Cancer Cells. *Biomacromolecules* **2014**, *15* (7), 2629−2641.
(24) Klumperman, B. Free radical copolymerization of styrene and maleic anhydride: kinetic studies at low and intermediate conversion. Technische Universiteit Eindhoven, 1994.
(25) Craig, A. F.; Clark, E. E.; Sahu, I. D.; Zhang, R. F.; Frantz, N. D.; Al-Abdul-Wahid, M. S.; Dabney-Smith, C.; Konkolewicz, D.; Lorigan, G. A. Tuning the size of styrene-maleic acid copolymer-lipid nanoparticles (SMALPs) using RAFT polymerization for biophysical studies. *Biochim. Biophys. Acta, Biomembr.* **2016**, *1858* (11), 2931−2939.
(26) Xu, T.; Zhao, N. N.; Ren, F.; Hourani, R.; Lee, M. T.; Shu, J. Y.; Mao, S.; Helms, B. A. Subnanometer Porous Thin Films by the Co-assembly of Nanotube Subunits and Block Copolymers. *ACS Nano* **2011**, *5* (2), 1376−1384.
(27) Presley, A. D.; Chang, J. J.; Xu, T. Directed co-assembly of heme proteins with amphiphilic block copolymers toward functional biomolecular materials. *Soft Matter* **2011**, *7* (1), 172−179.
(28) Zhao, Y.; Thorkelsson, K.; Mastroianni, A. J.; Schilling, T.; Luther, J. M.; Rancatore, B. J.; Matsunaga, K.; Jinnai, H.; Wu, Y.; Poulsen, D.; Frechet, J. M. J.; Alivisatos, A. P.; Xu, T. Small-molecule-directed nanoparticle assembly towards stimuli-responsive nanocomposites. *Nat. Mater.* **2009**, *8* (12), 979−985.
(29) Xu, T.; Shu, J. Coiled-coil helix bundle, a peptide tertiary structural motif toward hybrid functional materials. *Soft Matter* **2010**, *6* (2), 212−217.
(30) Harrisson, S.; Ercole, F.; Muir, B. W. Living spontaneous gradient copolymers of acrylic acid and styrene: one-pot synthesis of pH-responsive amphiphiles. *Polym. Chem.* **2010**, *1* (3), 326−332.
(31) Gody, G.; Zetterlund, P. B.; Perrier, S.; Harrisson, S. The limits of precision monomer placement in chain growth polymerization. *Nat. Commun.* **2016**, *7*, 10514.
(32) van den Dungen, E. T. A.; Rinquest, J.; Pretorius, N. O.; McKenzie, J. M.; McLeary, J. B.; Sanderson, R. D.; Klumperman, B. Investigation into the initialization behaviour of RAFT-mediated styrene-maleic anhydride copolymerizations. *Aust. J. Chem.* **2006**, *59* (10), 742−748.
(33) Edelstein, A.; Amodaj, N.; Hoover, K.; Vale, R.; Stuurman, N. Computer control of microscopes using microManager. *Curr. Protoc Mol. Biol.* **2010**, 14.20.
(34) Mayo, F. R.; Lewis, F. M. Copolymerization I A basis for comparing the behavior of monomers in copolymerization, the copolymerization of styrene and methyl methacrylate. *J. Am. Chem. Soc.* **1944**, *66*, 1594−1601.
(35) Chernikova, E.; Terpugova, P.; Bui, C. O.; Charleux, B. Effect of comonomer composition on the controlled free-radical copolymerization of styrene and maleic anhydride by reversible addition-fragmentation chain transfer (RAFT). *Polymer* **2003**, *44* (15), 4101−4107.
(36) Lindhoud, S.; Carvalho, V.; Pronk, J. W.; Aubin-Tam, M. E. SMA-SH: Modified Styrene-Maleic Acid Copolymer for Functionalization of Lipid Nanodiscs. *Biomacromolecules* **2016**, *17* (4), 1516−1522.
(37) Abel, B. A.; McCormick, C. L. "One-Pot" Aminolysis/Thiol Maleimide End-Group Functionalization of RAFT Polymers: Identifying and Preventing Michael Addition Side Reactions. *Macromolecules* **2016**, *49* (17), 6193−6202.

DOI: 10.1021/acs.biomac.7b01136
Biomacromolecules XXXX, XXX, XXX−XXX